High Speed Bearing Wear Rate Measurements for Spacecraft Active Thermal Control Fluid Pumps with a Novel Pin on Disk Apparatus

Robert J. Bruckner* and Richard A. Manco II**

Abstract

A novel pin on disc tribometer was designed and constructed to generate a high-speed, wear coefficient database for hydrodynamic bearings that are typically used in canned motors found in the active thermal control circuits of robotic and inhabited spacecraft. The primary motivation for this work was the premature failure of the active external thermal control pump on the International Space Station in 2010. During the failure investigation of this incident, the root cause was postulated to be high speed wear of the bearings. Although a detailed forensic analysis gave credibility to this theory, the lack of wear coefficient data at relevant conditions prevented validation of this finding. The database generated from the new Extreme Environment Tribometer (EET) enabled a closure calculation within 5% of the observed wear from inspections of the failed hardware. Testing in anhydrous ammonia and surrogate fluid was performed to provide a means for simplified testing in the future and to populate a preliminary database for the design of future active thermal control systems on spacecraft. The EET and test techniques developed for the measurement of high-speed wear coefficients are available to future system designers.

Introduction

Active thermal control systems on spacecraft, both robotic and inhabited, most commonly rely upon a high speed canned motor pump to circulate the heat transfer fluid between heat exchangers and radiators. Three notable NASA examples of spacecraft with such pumps are the Parker Solar Probe, the Orion Crew Module, and the International Space Station [1-10]. A graphical representation of a canned motor pump is shown in figure 1 [11,12]. The working fluid in figure 1 is colored light blue and highlights the most unique feature of the pump. This feature includes the use of the primary working fluid as the hydrodynamic bearing lubricant and the heat transfer medium to remove eddy current losses from the rotating group. The primary reason for the use of canned motor pumps in spacecraft is the elimination of high speed shaft seals, which are the most likely cause of failures in traditional pump designs. The canned motor pump has become ubiquitous not only in spacecraft active thermal management but also in ground based applications where high reliability and an intolerance to working fluid contamination are key design constraints. While these pumps are elegant in their dual use of working fluid, this feature bring with it two key complications. First, the entire motor (rotor and stator) must be internally shrouded from the working fluid to protect electromagnetic components from the primary working fluid. Secondly, the characteristics of an excellent heat transfer fluid are in stark contrast to the optimum rheology required of lubricants for hydrodynamic bearings. A third complication arises from the use of these pumps in micro-gravity applications, such that the primary force on the bearings is not determined by gravity and the weight of the rotor. In ground-based applications this preferential load direction is used to identify the critical bearing locations and to incorporate health monitoring instrumentation to determine incipient failure of the bearings due to high wear.

* NASA Glenn Research Center, Cleveland, Ohio

** HX5 Sierra at NASA Glenn Research Center, Cleveland, Ohio

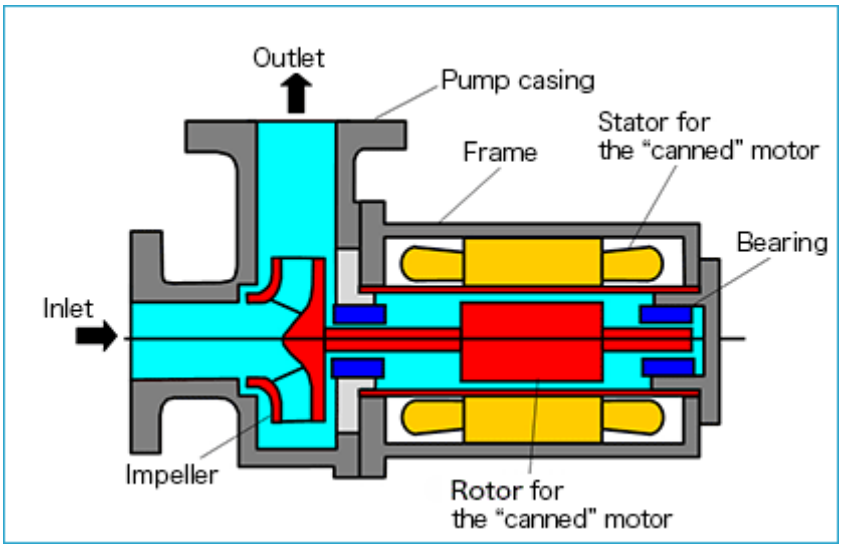

Figure 1. A typical high speed canned motor pump.

These complicating factors aligned in an unfortunate way on the International Space Station in 2010 and led to the premature failure of one of two active thermal control pumps used to maintain heat balance within the habitable volume. A failure investigation on this pump indicated that extreme wear of the bearings was the root cause due to operation beyond the hydrodynamic load capacity of the bearing. A complete description of this failure and early operational recovery efforts has been documented in [13].

This failure triggered an extensive study of the wear rates for this bearing material in relevant environments. An experimental approach was taken for this investigation due to the high rubbing speed and flooded, liquid condition at which this wear occurs. A new experimental apparatus was designed, constructed and operated to generate a database of relevant wear rate coefficients suitable for predicting wear life of high speed canned motor pumps in operating microgravity conditions. The apparatus, known as the Extreme Environment Tribometer (EET). It includes an operating temperature range of -68 to 65 C(-90 to 150 F), pressure range from 6.9 to 2585. kPa (1 to 375 psia), and rubbing speeds up to 25 mps (81 fps). It was designed to operate in 100% anhydrous ammonia and therefore will also accommodate both the new class of designer heat transfer fluids with anti-corrosion additives as well as the traditional heat transfer fluids such and propylene glycol and water.

Wear in Hydrodynamic Bearings

Hydrodynamic bearings, such as those commonly used in canned motor pumps, experience wear at both high speed and low speed operation. Low speed wear is primarily experienced during startup and shutdown of the rotating system. Figure 2 has been reproduced from [13] to demonstrate this phenomenon. At low rotational speeds the shaft contacts the static bearing until the mixed lubrication regime is reached. As speed is increased further, beyond the mixed lubrication region, the bearings operate in a non-contacting or hydrodynamic mode. In this mode, no wear occurs and the surfaces are separated by a thin layer of lubricant, or working fluid in the case of a canned motor pump. In the low speed phase of operation, solid surface contact occurs and a wear condition may exist. Typically, the static bearing material is selected to tolerate this wear while the shaft in the bearing location is prepared

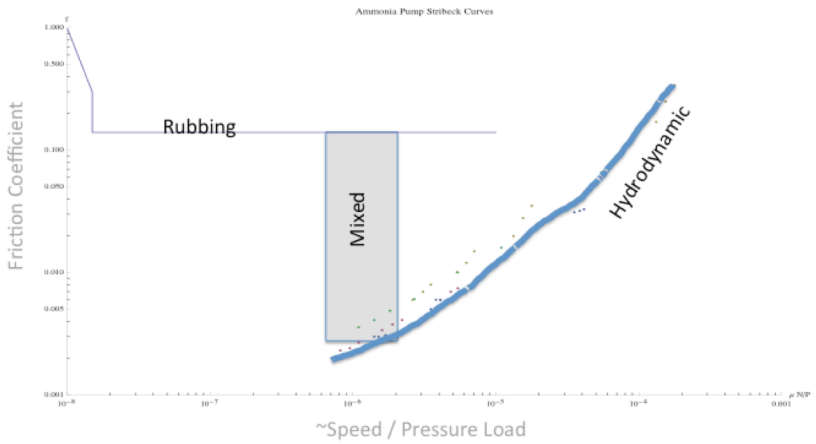

Figure 2. The Stribeck Curve for the Hydrodynamic Bearing.

with a hard coating having a very low surface roughness. This low speed wear condition is a well understood phenomenon and wear coefficient data of various bearing and shaft coating combinations is readily available. Even if the data is not readily available, wear coefficient data at low speeds can be obtained from a test program conducted on a large number of commercially available pin-on-disc or block-on-ring tribometers. In fact, in the early phases of the work described herein, low speed wear coefficient data was generated to gain an understanding of the wear couple at hand.

High speed wear on hydrodynamic bearings is a unique phenomenon and can only occur when the load capacity of a bearing is exceeded at high speed. This situation occurred on the cooling pumps of the International Space Station (ISS) in 2010 and triggered the premature shutdown of one of the pumps. Although in this situation the weight of the rotor was not present due to operation in a microgravity environment, secondary forces aligned to overcome the non-contacting load capacity of the bearing leading to severe and unexpected wear. The phenomenon of high speed wear has not been studied in the application to hydrodynamic bearings, and this phenomenon is unique to niche applications such as microgravity operation. Wear mechanisms and material wear coefficients in this region require a test based approach to quantify the functional life of a bearing which experiences these conditions.

The Extreme Environment Tribometer (EET)

Design

A survey of commercial and custom designed research tribometers was conducted in order to identify a test rig that could meet the needs of the current test program [14-20]. No such apparatus was identified, which triggered a new tribometer design effort. The EET was designed with the following characteristics, which were required to conduct high-fidelity wear coefficient measurements in conditions that matched those in the ISS cooling pump bearings:

- Pin-on-disc configuration with modular running gear and test chamber capable of block-on-ring or hydrodynamic testing.
- Capable of high rubbing speeds that spanned the front and rear journal bearing design space.
- Flooded liquid operation at the rubbing contact points with liquids that are unfriendly to many materials, specifically anhydrous liquid ammonia.
- Vacuum and elevated pressure capabilities to enable test operation with liquids that are not thermodynamically stable at standard temperature and pressure (STP).
- Constant temperature operation during test operations.

The final design of the EET is shown in Figures 3 and 4. The design consists of a pressure vessel that houses a vertical, rotating shaft supported on dry, unlubricated rolling element bearings. The use of unlubricated bearings was paramount to the successful creation of the wear coefficient database, since contamination of the test fluid, anhydrous ammonia in this case, by the oils or greases in the rolling element bearings would invalidate the data applicability to the ISS wear conditions. Additionally, the high pH of the anhydrous ammonia would likely degrade conventional lubricants, cage materials, and steels. Ball bearings that were made with ceramic zirconia races, zirconia balls, and a polytetrafluoroethylene (PTFE) cage were used in this application. A key EET running gear design feature was the elimination of inner race radial interference fits. A purely axial preload was used to maintain shaft bearing interface alignment and eliminate potential slip through the use of an axial spring pack. This configuration enabled the ceramic to be placed in compression during all phases of assembly and operation and eliminated the ceramic bearing tensile stresses at the inner race failure mode.

Mounted to the rotating shaft bottom was the disc. The disc was 100 mm in diameter, and each disc was manufactured with a hard chrome coating polished to a 0.1-μm surface finish, the same specification as is typical in rotor bearing surfaces.

Below the rotating disc was the test chamber, which consisted of a four-pin load block. Each pin ran on its own wear track, which enabled four data points at unique speeds to be obtained with each test operation. Contact load between the carbon pins and the rotating disc was maintained by a spring pack and a load screw arrangement whose features were machined into the load block.

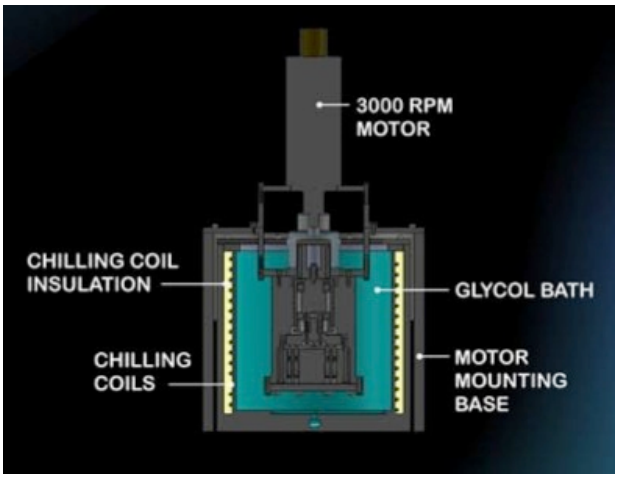

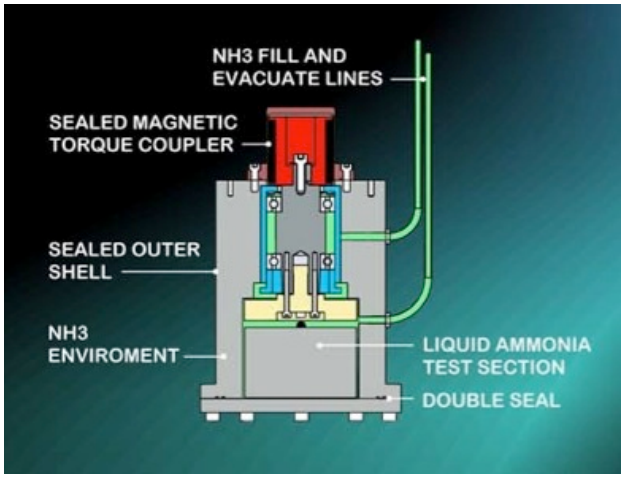

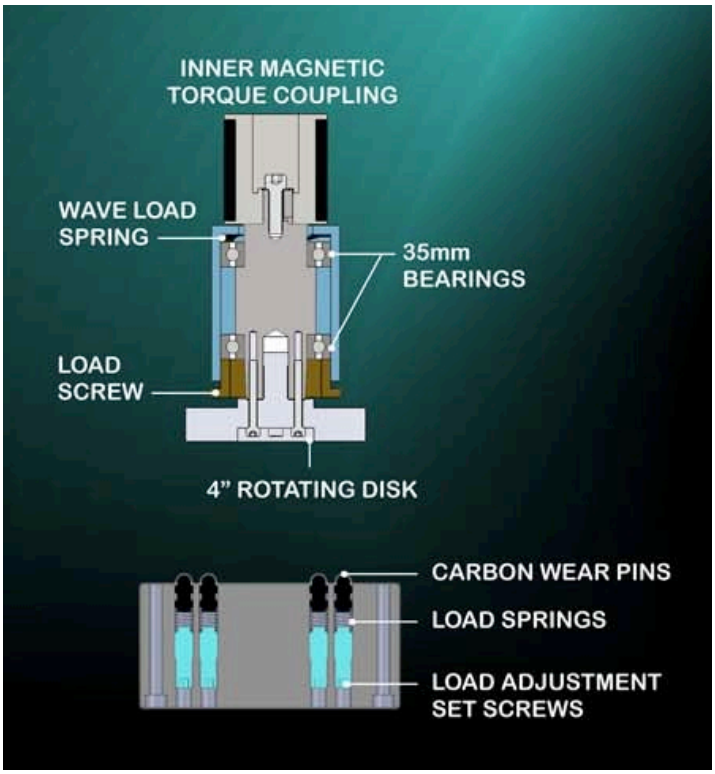

Figure 3. EET Design

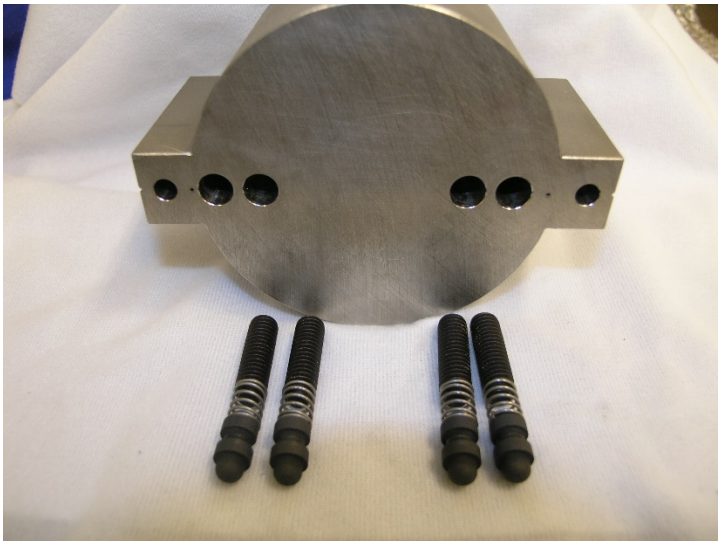

Figure 4. EET and Test Specimens

The entire pin-on-disc arrangement was enclosed in a pressure vessel to enable safe operation in a thermodynamically controlled environment. A motor was mounted on the pressure vessel top, and torque was transferred to the shaft through a magnetic coupling. Three types of materials were used for the magnetic coupling dome to manage operational risk with eddy current heating of the pressure vessel. Design calculations and operational experience provided the following constraints:

- Stainless steel dome: use to 300 rpm.
- Titanium dome: use to 900 rpm.
- Glass-filled polyetheretherketone (PEEK) dome: use to 3,500 rpm.

To maintain a constant temperature during test operations and to enable tribometer precooling or preheating to simplify liquid filling operations, a thermal bath was constructed in which the sealed tribometer could be submerged. This thermal chamber was designed to meet a –75 to +125 °C temperature range.

Operation

The procedure for operation of the EET was as follows:

- Test Specimen Preparation
- Perform pretest photomicroscopy and profilometry of the chrome-coated disc and four carbon pins to document pretest configuration.
- Install runner onto the shaft and verify axial runout is less than 12.6 μm.
- Verify motor operation, magnetic coupling alignment, and set speed point in motor controller.
- Install carbon pins in PTFE sabot and set spring preload.
- Measure and record pretest spring preload for each pin.
- Install load block into pressure.
- Install bottom seal and flange.
- Environmental Control
- Prepare the constant temperature bath with appropriate heaters, chillers, and heat transfer fluids.
- Immerse the tribometer in the temperature-controlled bath.
- Monitor internal temperature of the EET through purge gas exit temperature.
- At the desired temperature, fill the EET with a predetermined volume of test fluid.
- Monitor the tribometer and fill vessel mass, and the EET pressure and temperature.
- After pressure, temperature, and fluid levels have stabilized, initiate test.
- Test Operation
- During startup, monitor motor speed to ensure proper operation.
- Continuously record motor speed and power draw at a minimum of 10 Hz.
- Verify motor speed with external strobe every 10 minutes.
- Monitor pressure, temperature, and speed for stability and trends.
- Terminate the test at the first onset of unexpected or unexplained variability in test conditions.
- Terminate test at the desired sliding distance (time).
- Collect post-test data.
- Drain test liquid from test chamber and collect in specimen jar and any debris.

- Purge test chamber with nitrogen and bring to room temperature while monitoring pressure temperature and gas exit conditions.
- When safe conditions exist within the tribometer, remove the lower flange and seal.
- Remove the load block.
- Measure and record the post-test normal force on each carbon pin.
- Perform photomicroscopy, profilometry, debris analysis, and additional diagnostics as the test conditions or results dictate.

Wear Coefficient Data

Low speed Wear Data

In order to build an early database of wear coefficients while the EET was under fabrication and to gain experience with the material couple, a series of low speed wear tests were performed on commercial pin on disc tribometers in both dry and flooded contact conditions. A photograph of typical test hardware is shown in figure 5 and results are captured in table 1. Test results indicated a wear coefficient on the order of 10–7 (mm3/N m) with strong sensitivity to contact area (i.e., pressure). The wear coefficient is defined as cubic millimeters of worn material normalized by normal force (N) and sliding distance (m). The friction coefficient of the wear couple was measured in these tests to be in the range of 0.14 to 0.22 in room temperature air. Testing in flooded liquid conditions revealed a reduction of friction coefficient to the range of 0.07 to 0.11 while the wear coefficient remained within the same order of magnitude.

Figure 5. Test Specimens for low speed wear testing

EET Validation – Dry

Preliminary EET testing was conducted at STP conditions to establish operating procedures and confirm traceability to low speed testing. Once the traceability and operating procedures were established, the EET was operated at high speeds to expand the wear coefficient database. A summary of pertinent wear coefficient data for both low- and high-speed EET operation in air is included in Table 2. High-speed wear coefficients measured in air at ambient conditions were equivalent to those measured on the commercial tribometers. This provided confidence in the EET design and operation.

Surrogate Fluid Wear Coefficient

The wear coefficient database was expanded to include flooded liquid conditions at high speeds. Initially, water was used in the high-speed flooded liquid tests. These initial tests uncovered a nontrivial issue in the test operation. Hydrodynamic lift was being generated between the carbon pin to chrome runner interface. This lift was the result of several factors, including low axial runout in the rotating disk, low surface roughness on the chrome, low surface roughness on the worn carbon bearing material, high absolute viscosity of the water at room temperature, and relatively high speeds. During the testing initial phase, wear was observed during the initial (i.e., high contact pressure) phase of pin wear. It was postulated that even at relatively high contact pressures the pin-disc interface could develop sufficient hydrodynamic lift to prevent further wear. To overcome this limitation for high-speed flooded operation, several modified test techniques were developed without success to disrupt the hydrodynamic film. The only reliable technique for eliminating hydrodynamic lift in these tests was reduction of the absolute fluid viscosity through elevated temperature.

Once an acceptable test technique was developed, surrogate fluid testing was conducted. Water, 4 percent ammonia in water, and 28 percent ammonia in water solutions were tested at temperatures below their boiling points. The evolution of wear coefficient with reduced contact pressure was tracked during this test campaign. A summary of the test data is included in Table 2.

Anhydrous Ammonia Measured Wear Coefficients

The final phase of testing on the EET encompassed the exact conditions found in the failed ISS pump from 2010, high contact speeds in flooded anhydrous ammonia. Data is presented in table 3 along with data for a 28% ammonia in water mixture and bone-dry, gaseous nitrogen at -45C.

The wear coefficient database enables calculations to be performed to evaluate the failure progression theory for the ISS active thermal control pump. By combining the available on-orbit operations data from the of the failed pump with the new wear coefficient database, the closure calculation was within 5% of the observed wear found during the failure investigation. This compares to calculations based on estimates of wear coefficients that ranged from -98% to over 5 times the observed wear volume.

Cold, Dry Material Performance

One final set of tests was conducted after the anhydrous ammonia data were obtained. The objective of this test was to evaluate the effect of low temperature on the wear rates because the EET was operated at approximately –45 °C during the anhydrous ammonia tests to keep the internal pressure low and minimize the risk of a thermal runaway and boil-off situation. The final cold test was conducted in a dry gaseous nitrogen environment at –45 °C. The measured wear coefficients were three orders of magnitude higher than those measured in the flooded anhydrous ammonia tests. Three potential causes for these high wear coefficients were postulated. The resin binding the graphitic carbon could go through a secondary glass transition temperature, causing embrittlement. The differential thermal expansion between resin and carbon may cause stress cracking and induce a weaker composite material. The surface layer of the carbon in rubbing contact may be highly sensitive to humidity and trace hydrogen.

The first theory was investigated with differential calorimetry. Specimens were sent to a polymers lab to search for an embrittlement temperature between room temperature and –100 °C. None were found.

The second theory of differential thermal expansion causing microcrack formation at the resin-carbon bond was investigated using two methods. First, high-power microscopy was used to search for cracks, but none were observed. The second technique was to continue testing the specimens in ambient conditions. At ambient conditions, the measured wear coefficients returned to normal levels, which indicated that a reversible phenomenon was occurring, thus eliminating the microcracking theory.

The third cause of the high wear rate coefficients was investigated by testing in dry nitrogen gas at ambient temperatures. Under these conditions, the high wear rates were repeated, which gave credibility to the sensitivity of this material to humidity and trace hydrogen to achieve low wear rates.

Discussion

A new pin on disc apparatus was designed and fabricated to provide high speed wear coefficient data for hydrodynamic bearings in canned motors. These motors and bearing arrangements are commonly used in actively pump thermal control circuits for manned and robotic spacecraft. The dramatic increase in desired life of these pumps has led to the need to understand the high speed wear phenomenon of the bearings. Test data in surrogate fluids has reveal important trends in the wear coefficients. Surrogate fluids are significant because they may ease the burden of testing and provide a level of similarity between different coolants used in various spacecraft. The significant trends include:

- Twenty-eight percent ammonia hydrate solution is a suitable surrogate fluid for 100 percent anhydrous ammonia for the material wear couple present in the PCVP bearings.
- Four percent ammonia hydrate solution behaves similarly to pure water for the material wear couple present in the PCVP bearings.
- Wear rates measured in water are two orders of magnitude higher than wear rates measured in anhydrous ammonia.
- Wear rates measured in dry nitrogen gas were two orders of magnitude higher than those measured in air at ambient temperature, pressure, and humidity.
- At rubbing speeds greater than 4 m/s, the wear rate decreased with increasing speed for flooded ammonia conditions.
- Based on testing, the high-speed wear coefficient of the ISS pump bearings to be in the range of 1.4 to 8.3E-09 (mm^3/(N m)).

Additionally, certain best practices were determined to be useful for future, long duration canned motor bearing designs.

- Document the bearing groove orientations with respect to key motor housing features if bearing pads are used.
- Preclude the secondary flow paths from generating rotor-bearing asymmetric loading.
- Maintain a symmetric journal bearing design to the greatest extent possible.

The EET and the test technique developed to measure high speed wear coefficients is available to future spaceflight programs that may utilize actively pumped thermal control circuits. Furthermore, the database generated from the initial EET test program was able to validate the failure mode of the 2010 ISS thermal control pump failure to within 5% of the observed material loss, which was measured during the failure investigation. This significant improvement in the closure calculations have provided increased confidence in the wear progression and the recovery procedures for the ISS thermal control system.

References

1. Birur, G. C., Bhandari, P., Gram, M. B., and Durkee, J., "Integrated Pump Assembly – An Active Cooling System for Mars Pathfinder Thermal Control," Society of Automotive Engineers, 26th International Conference on Environmental Sciences, Monterey, CA, 1996.
2. Lockwood, M. K., Ercol, C. J., Cho, W. L., Hartman, D., and Adamson, G., "An Active Cooling System for the Solar Probe Power System," AIAA, International Conference on Environmental Systems, AIAA-2010-6294, 2010.
3. Swanson, T. D. and Birur, G. C., "NASA Thermal Control Technologies for Robotic Spacecraft," National Aeronautics and Space Administration, N20030031332, 2003.
4. Westheimer, D. T. and Tuan, G. C., "Active Thermal Control System Considerations for the Next Generation of Human Rated Space Vehicles," AIAA AeroSpace Sciences Meeting, AIAA-2005-342, 2005.
5. Paris, A. D., Bhandari, P., and Birur, G. C., "High Temperature Mechanically Pumped Fluid Loop for Space Applications – Working Fluid Selection," SAE International, 04ICES-282, 2004.
6. Shen, F., Drolen, B., Prabhu, J., Harper, L., Eichinger, E., and Hgyuen, C., "Long Life Mechanical Fluid Pump for Space Applications," AIAA AeroSpace Sciences Meeting, AIAA-2005-273, 2005.
7. Baldauf, R. W., Kawecki, T., Purdy, W., and Hoang, T. T., "Development of a Bearingless Ammonia Pump for Spacecraft Thermal Control," NRL Review, 2008.
8. Shen, F., Drolen, B., Prabhu, J., Harper, L., Eichinger, E., Nguyen, C., "Long Life Mechanical Fluid Pump for Space Applications," 43rd AIAA Aerospace Sciences Meeting, AIAA-2005-273, January 10-13, 2005
9. Lockwood, M. K., Ercol, C. J., Cho, W. L., Hartman, D., and Adamson, G., "An Active Cooling System for the Solar Probe Power System," AIAA 40th International Conference on Environmental Systems, AIAA-2010-6294, 2010.
10. Paris, A. D., Bhandari, P., and Birur, G. C., "High Temperature Mechanically Pumped Fluid Loop for Space Applications – Working Fluid Selection," SAE International, 04ICES-282, 2004.
11. Bloch, P. E., "Understanding Canned Motor Pumps," Maintenance Technology, September 1, 2008.
12. Foszcz, J. L., "Canned Motor Pumps," *Plant Engineering*, June 3, 1993.
13. Bruckner, R.J., Manco R. A., "ISS Ammonia Pump Failure, Recovery, and Lesson Learned – A Hydrodynamic Bearing Perspective", Prodeedings of the 42nd Aerospace Mechanisms Symposium, NASA Goddard Space Flight Center, May 14-16, 2014.

14. Jeon, H. G., Lee and Y. Z., "The Evaluation of Wear Life Based on Accelerated Test through Analysis of Correlation between Wear Rate and Lubricant Film Parameter," *Tribology Transactions*, February 19, 2013.
15. ASTM International, "Standard Test Method for Wear Testing with a Pin-on-Disk Apparatus," G99-05, reapproved 2010.
16. Gomes, J. R., Silva, O. M., Silva, C. M., Pardini, L. C., and Silva, R. F., "The Effect of Sliding Speed and Temperature on the Tribological Behavior of Carbon-carbon Composites," *Wear*, Elsevier, Vol. 249, pp. 240–245, 2001.
17. Lancaster, J. K., "Dry Bearings: A Survey of Materials and Factors Affecting their Performance," *Tribology*, December 1973.
18. Midgley, J. W. and Teer, D. G., "An Investigation of the Mechanism of the Friction and Wear of Carbon," Transactions of the American Society of Mechanical Engineers (ASME), December 1963.
19. Sliney, H. E. and Jacobson, T. P., "Some Effects of Composition on the Friction and Wear of Graphite Fiber Reinforced Polyimide Liners in Plain Spherical Bearings," NASA Technical paper 1229, 1997.
20. Demas, N. G. and Polycarpu, A. A., "Ultra High Pressure Tribometer for Testing CO2 Refrigerant at Chamber Pressures up to 2,000 psi to Simulate Compressor Conditions," *Tribology Transactions*, Vol. 49, pp. 291–296, 2006.

Table 1 Wear Coefficient Data from Low-speed Tribometer

Fluid	Load (N)	Linear Speed	Wear Coefficient (mm^3/N-m)	Sample Temperature	Contact Pressure (Mpa)
4% NH_3 Hydrate	10	100 mm/s	4.97865E-07	25.5 to 27 C	2.601
4% NH_3 Hydrate	10	200 mm/s	2.41698E-07	25.5 to 27 C	3.581
4% NH_3 Hydrate	10	200 mm/s	2.95354E-07	25.5 to 27 C	1.798
dry, air	10	300 mm/s	6.38E-07	25.5 to 27 C	12.109
dry, air	10	300 mm/s	1.29384E-07	25.5 to 27 C	8.416
dry, air	10	900 mm/s	1.83617E-07	25.5 to 27 C	6.466
dry, air	10	900 mm/s	1.92718E-07	25.5 to 27 C	7.101
proplyene glycol	5	300 mm/s	2.39490E-08	25.5 to 27 C	8.043
dry, air	2	900 mm/s	1.57290E-07	25.5 to 27 C	1.378
dry, air	1	900 mm/s	1.33452E-07	25.5 to 27 C	0.842
4% NH_3 Hydrate	10	100 mm/s	3.23704E-07	25.5 to 27 C	2.011
4% NH_3 Hydrate	10	600 mm/s	3.29972E-08	25.5 to 27 C	7.082
4% NH_3 Hydrate	10	400 mm/s	8.03432E-08	25.5 to 27 C	4.744
dry, air	10	600 mm/s	3.54035E-07	25.5 to 27 C	2.244
dry, air	10	400 mm/s	1.67E-07	25.5 to 27 C	3.393

	Pin A			Pin B			Pin C			Pin D				
Test Date	Motor Speed (rpm)	Sliding Speed (m/s)	Wear Coeff (m³/N-m)	Motor Speed (rpm)	Sliding Speed (m/s)	Wear Coeff (m³/N-m)	Motor Speed (rpm)	Sliding Speed (m/s)	Wear Coeff (m³/N-m)	Motor Speed (rpm)	Sliding Speed (m/s)	Wear Coeff (m³/N-m)	Temperature, C	Pressure
10-Mar	901.9	4.1982	2.57E-07	901.9	2.9987	6.32E-07	901.9	2.3999	1.18E-06	901.9	3.5984	8.19E-07	52-59	ambient
		4.1982	2.63E-07		2.9987	6.37E-07		2.3989	1.16E-06		3.5984	8.30E-07	52-59	ambient
17-Mar	902.6	4.2014	1.74E-07	902.6	3.0010	1.58E-07	902.6	2.4008	6.17E-07	902.6	3.6012	4.45E-07	52-59	ambient
		4.2014	1.60E-07		3.0010	4.46E-07		2.4008	6.75E-07		3.6012	4.47E-07	52-59	ambient
18-Mar	600	2.7929	1.66E-07	600	1.9949	4.48E-07	600	1.5959	5.27E-07	600	2.3939	3.95E-07	52-59	ambient
		2.7929	1.59E-07		1.9949	4.57E-07		1.5959	4.95E-07		2.3939	4.03E-07	52-59	ambient
20-Mar	300.6	1.3992	1.76E-07	300.6	0.9995	2.74E-07	300.6	0.7996	3.02E-07	300.6	1.1993	2.93E-07	52-59	ambient
		1.3992	1.90E-07		0.9995	3.10E-07		0.7996	3.80E-07		1.1993	2.30E-07	52-59	ambient
25-Mar	303.1	1.4109	2.29E-07	303.1	1.0078	2.53E-07	303.1	0.8062	1.11E-07	303.1	1.2093	1.18E-07	52-59	ambient
		1.4109	2.61E-07		1.0078	2.27E-07		0.8062	1.05E-07		1.2093	1.86E-07	52-59	ambient
27-Mar	901.8	4.1977	7.09E-08	901.8	2.9984	9.70E-08	901.8	2.3987	2.78E-07	901.8	3.5980	2.05E-07	52-59	ambient
		4.1977	5.45E-08		2.9984	7.17E-08		2.3987	2.78E-07		3.5980	2.15E-07	52-59	ambient
31-Mar	302.9	1.4099	1.87E-07	302.9	1.0071	4.05E-07	302.9	0.8057	5.60E-07	302.9	1.2085	3.95E-07	95-98	ambient
		1.4099	2.27E-07		1.0071	4.46E-07		0.8057	5.76E-07		1.2085	4.09E-07	95-99	ambient
1-Apr	301.2	1.4020	5.19E-08	301.2	1.0014	1.51E-07	301.2	0.8012	1.74E-07	301.2	1.2017	1.79E-07	95-100	ambient
		1.4020	4.02E-08		1.0014	1.45E-07		0.8012	1.94E-07		1.2017	1.72E-07	95-101	ambient
7-Apr	302.7	1.4090	7.18E-08	302.7	1.0064	5.83E-08	302.7	0.8051	1.09E-07	302.7	1.2077	6.44E-08	95-102	ambient
		1.4090	7.54E-08		1.0064	5.66E-08		0.8051	1.02E-07		1.2077	7.67E-08	95-103	ambient
9-Apr	600.5	2.7952	5.98E-08	600.5	1.9966	4.94E-08	600.5	1.5973	4.97E-08	600.5	2.3959	5.63E-08	95-104	ambient
		2.7952	5.55E-08		1.9966	6.77E-08		1.5973	4.18E-08		2.3959	4.54E-08	95-105	ambient
10-Apr	605.3	2.8175	8.11E-08	605.3	2.0125	1.12E-07	605.3	1.6100	1.25E-07	605.3	2.4150	9.20E-08	95-106	ambient
		2.8175	7.23E-08		2.0125	1.12E-07		1.6100	1.39E-07	0	2.4150	1.05E-07	95-107	ambient
13-Apr	903.7	4.2065	4.99E-08	903.7	3.0047	5.63E-08	903.7	2.4037	6.55E-08	903.7	3.6056	1.35E-07	95-108	ambient
		4.2065	6.70E-08		3.0047	2.94E-08		2.4037	6.98E-08		3.6056	1.34E-07	95-109	ambient
14-Apr	903.7	4.2065	5.74E-08	903.7	3.0047	1.11E-07	903.7	2.4037	1.79E-07	903.7	3.6056	1.09E-07	95-110	ambient
		4.2065	5.17E-08		3.0047	1.33E-07		2.4037	1.85E-07		3.6056	1.25E-07	95-111	ambient
15-Apr	1200.1	5.5862	3.11E-08	1200.1	3.9902	1.35E-07	1200.1	3.1921	1.83E-07	1200.1	4.7882	1.35E-07	95-112	ambient
		5.5862	3.20E-08		3.9902	1.22E-07		3.1921	1.60E-07		4.7882	1.23E-07	95-113	ambient
16-Apr	1200.1	5.5862	2.02E-08	1200.1	3.9902	6.77E-08	1200.1	3.1921	3.85E-08	1200.1	4.7882	1.32E-08	95-114	ambient
		5.5862	2.46E-08		3.9902	7.60E-08		3.1921	6.96E-08		4.7882	1.04E-08	95-115	ambient
17-Apr	1510.1	7.0292	2.68E-08	1510.1	5.0209	4.55E-08	1510.1	4.0167	1.18E-07	1510.1	6.0250	8.10E-08	95-116	ambient
		7.0292	2.59E-08		5.0209	4.41E-08		4.0167	1.14E-07		6.0250	8.28E-08	95-117	ambient

Table 2. Wear Coefficient Data Using 4 Percent Ammonium Hydrate Surrogate Fluid

Table 3. Wear Coefficient Data for 28 Percent Ammonia, 100 Percent Ammonia, and Dry Nitrogen Environments

Fluid	Linear Speed, m/s	Test pressure (psig)	Test temperature, C	Contact Pressure (Mpa)	ear Coefficient (mm^3/N-r
28% NH3	1.07	6.0-7.5	45	32	9.00E-09
28% NH3	1.33	6.0-7.6	46	29	8.00E-09
28% NH3	1.6	6.0-7.7	47	9.8	8.50E-09
28% NH3	1.87	6.0-7.8	48	20	6.50E-09
100% NH3	3.3	15	-43	31	6.20E-09
100% NH3	4.16	15	-43	29	8.30E-09
100% NH3	4.98	15	-43	20	5.40E-09
100% NH3	5.8	15	-43	21	8.30E-09
100% NH3	4.85	20	-43	22	6.90E-09
100% NH3	4.85	20	-43	23	3.10E-09
100% NH3	6.06	20	-43	34	2.33E-09
100% NH3	6.06	20	-43	28	1.69E-09
100% NH3	7.27	20	-43	34	1.99E-09
100% NH3	7.27	20	-43	22	2.47E-09
100% NH3	8.48	20	-43	35	1.48E-09
100% NH3	8.48	20	-43	26	1.38E-09
N2, bone dry	4.85	20	-45	21	7.15E-05
N2, bone dry	6.06	20	-45	21	4.99E-05
N2, bone dry	7.28	20	-45	21	3.85E-05
N2, bone dry	8.5	20	-45	21	2.19E-05